REPORT DOCUMENTATION PAGE

Form Approved
OMB No. 0704-0188

PLEASE DO NOT RETURN YOUR FORM TO THE ABOVE ORGANIZATION.

1. REPORT DATE *(DD-MM-YYYY)*	2. REPORT TYPE	3. DATES COVERED *(From - To)*
31-05-2010	Final	02-01-2007 to 01-31-2010

4. TITLE AND SUBTITLE
Computation and Modeling of Heat Transfer in Wall-Bounded Turbulent Flows

5a. CONTRACT NUMBER

5b. GRANT NUMBER
FA9550-07-1-0393

5c. PROGRAM ELEMENT NUMBER

6. AUTHOR(S)
Pasinato, Hugo D.

5d. PROJECT NUMBER

5e. TASK NUMBER

5f. WORK UNIT NUMBER

7. PERFORMING ORGANIZATION NAME(S) AND ADDRESS(ES)
Universidad Tecnologica Nacional-Facultad Regional Neuquen
Calle Pedro Rotter s/n
Plaza Huincul 8318, Argentina

8. PERFORMING ORGANIZATION REPORT NUMBER

9. SPONSORING/MONITORING AGENCY NAME(S) AND ADDRESS(ES)
Air Force Office of Scientific Research (AFOSR)

10. SPONSOR/MONITOR'S ACRONYM(S)

11. SPONSOR/MONITOR'S REPORT NUMBER(S)
AFRL-OSR-VA-TR-2012-0189

12. DISTRIBUTION/AVAILABILITY STATEMENT
Distribution A: public release

13. SUPPLEMENTARY NOTES
None

14. ABSTRACT

The dissimilarity between streamwise velocity and temperature in non-perturbed and perturbed turbulent channel and plane Couette flows was addressed using direct numerical simulations. The objective was to obtain insights that can aid turbulent heat-transfer modeling for non-equilibrium turbulent flows, based on the Reynolds stress. For perturbed flow different kind of perturbation like as blowing, suction, pressure gradient steps, etc, were used. It was found that, to some extent, the dissimilarity for both perturbed turbulent flow configurations(channel and Couette) are analogous, and that turbulence contribution to the mean-field dissimilarity was only a minor part in comparison with the contribution of pressure gradient. The contribution to dissimilarity by turbulence depends almost entirely on mean field dissimilarity. A simple transformation of the Reynolds stress can be used as a model for turbulent heat fluxes, which gives a reasonable a priori prediction of the heat fluxes in perturbed turbulent flows.

15. SUBJECT TERMS
Turbulent Heat Transfer; Velocity and Temperature Dissimilarity; Heat Transfer Modeling; Bounded Turbulent Flow; Direct Numerical Simulation.

16. SECURITY CLASSIFICATION OF:			17. LIMITATION OF ABSTRACT	18. NUMBER OF PAGES	19a. NAME OF RESPONSIBLE PERSON
a. REPORT	b. ABSTRACT	c. THIS PAGE			Pasinato, Hugo D.
UU	UU	UU		12	19b. TELEPHONE NUMBER *(Include area code)* 0054(299)4960510

AFOSR Final Performance Report

Contract/Grant Title: Computation and Modeling of Heat Transfer in Wall-Bounded Turbulent Flows

Grant Number: FA9550-07-1-0393

Reporting Period: 1 February 2007 to 31 January 2010

Principal Investigator: Dr. Hugo D. Pasinato

Chemical Engineering Department

Facultad Regional Neuquén

Universidad Tecnológica Nacional

Pedro Rotter s/n

8318-Plaza Huincul, Neuquén, Argentina

Phone:+54(299)4960510

Fax:+54(299)4963292

Cellphone:+54(299)155 555 794

I. Status of Effort

In this project the dissimilarity between streamwise velocity and temperature in developed or non-perturbed (where 'developed condition' means a region downstream of a point beyond which the flow field's behavior is streamwise invariant) and perturbed turbulent channel and plane Couette flows, was addressed using direct numerical simulations, DNS. The main goal of this study addressing the dissimilarity between streamwise velocity and temperature, was to obtain insights that can aid turbulent heat-transfer modeling based on Reynolds stress (Note that throughout this report the expression *mean-field dissimilarity* will be used for the difference $(U - \Theta)$ in dimensionless form, where U and Θ are the

mean streamwise velocity and temperature, respectively; *dissimilarity of streamwise velocity and temperature fluctuations* for the dimensionless difference $(u' - \theta')$; *streamwise turbulent flux dissimilarity* for the dimensionless difference $(\langle u'u' \rangle - \langle \theta'u' \rangle)$; and *wall-normal turbulent flux dissimilarity* for the dimensionless difference $(\langle u'v' \rangle - \langle \theta'v' \rangle)$).

First the natural dissimilarity of streamwise velocity and temperature fluctuations, in non-perturbed turbulent channel and plane Couette flows, was characterized (Kestin and Richardson, 1963; Fulachier and Dumas, 1976; Antonia et. al, 1987). For both of the flow configurations, a Reynolds number based on the friction velocity of about 150 was used (Pasinato, H.D., Velocity and temperature dissimilarity in fully developed turbulent channel and plane Couette Flows, *Int. J. Heat F. Flow*, **32**, pp. 11-25, 2011).

In the second part the dissimilarity between the mean turbulent fluxes of streamwise velocity and temperature in perturbed turbulent flows was characterized (Kong, Choi, and Lee, 2001). Numerical experiments for turbulent channel and plane Couette flows were implemented, with analogous mean streamwise velocities and temperatures in developed conditions, which were then perturbed in different ways in a second DNS. To provide inflow boundary conditions for the perturbed-developing flow, a parallel DNS with identical numerical resolution was performed. The perturbations used in the study were (a) local blowing or suction from a narrow span-wise slot at the walls, (b) local streamwise pressure-gradient steps, adverse and favorable, in a narrow span-wise volume in the buffer region, (c) local wall-normal pressure-gradient steps in a narrow span-wise volume in the buffer region, and (d) local wall temperature steps. The main idea was to study the disruption of mean-field similarity due to turbulence in perturbed turbulent flows and to study the main causes of dissimilarity of the turbulent fluxes for streamwise momentum and heat (Pasinato, H.D., Streamwise Velocity and Temperature Dissimilarity in Perturbed Channel and Plane Couette flows, to be submitted).

II. Accomplishments and New Findings

$=>$ It was found that the natural dissimilarities were more associated with those events in $(Q2 + Q4)$, according to the quadrant analysis technique (at about 60%) for both flow configurations. In other words, the same types of events responsible for wall-normal turbulent fluxes (streamwise momentum and heat) are also responsible in part for the dissimilarities.

$=>$ In the frequency domain it was shown that the dissimilarity is caused by a shift toward higher frequencies as the distance from the wall increases for the θ' spectrum in comparison with the u' spectrum.

=> At the wall-layer the θ' spectrum presented higher frequencies than u' and lower frequencies than p' (and also than $\partial p'/\partial x$ spectrum). These differences generate a more significant correlation of θ' with $\partial p'/\partial x$ than u' with $\partial p'/\partial x$. This correlation difference is the main cause of the dissimilarities in non-perturbed turbulent flows; or in the decorrelation of u' and θ' from the wall toward the central region.

=> For perturbed turbulent flow the dissimilarity for both flow configurations were analogous.

=> The contribution to the mean-field dissimilarity by turbulent fluxes dissimilarity was a minor part in comparison with the pressure gradient contribution.

=> The contribution to mean-field dissimilarity by the streamwise turbulent fluxes, $(\langle u'u'\rangle - \langle u'\theta'\rangle)$, mainly occurs in the perturbation region, while those due to wall-normal fluxes, $(\langle v'u'\rangle - \langle v'\theta'\rangle)$, occurs mostly downstream of the perturbation region.

=> The wall-normal turbulent fluxes make a greater contribution to mean-field dissimilarity than the streamwise fluxes.

=> The leading dissimilarity contributor to the wall-normal turbulent fluxes dissimilarity was $\langle v'v'\rangle \partial\Phi/\partial y$, where Φ is the difference $(U - \Theta)$.

=> A simple transformation of the Reynolds stresses in the streamwise and wall-normal direction, $\langle u'u'\rangle$, $\langle u'v'\rangle$, gives a reasonable *a prior* prediction of the turbulent heat fluxes $\langle \theta'u'\rangle$, $\langle \theta'v'\rangle$.

III. Natural dissimilarity in non-perturbed turbulent flows

(III.a) Definition of a new variable to measure dissimilarity

In the numerical experiments the streamwise velocity and temperature are analogous in the mean values (the Reynolds averaged conservation laws for streamwise velocity and temperature, with some restrictions as constant fluid properties, $Pr = 1$, and identical boundary conditions, are analogous). Thus $\phi = (U - \Theta) + (u' - \theta')$, resulting that $\phi = \Phi + \phi'$ as all variables, where the variance of ϕ' is

$$VAR(\phi') = (\phi^+)^2 = \langle u'u'\rangle - \langle u'\theta'\rangle + \langle \theta'\theta'\rangle - \langle u'\theta'\rangle. \quad (1)$$

The local variance $VAR(\phi')$ was used as a measure of the mean local dissimilarity and the averaged variance $VAR(\phi')_{ave}$ as an averaged value in the whole domain.

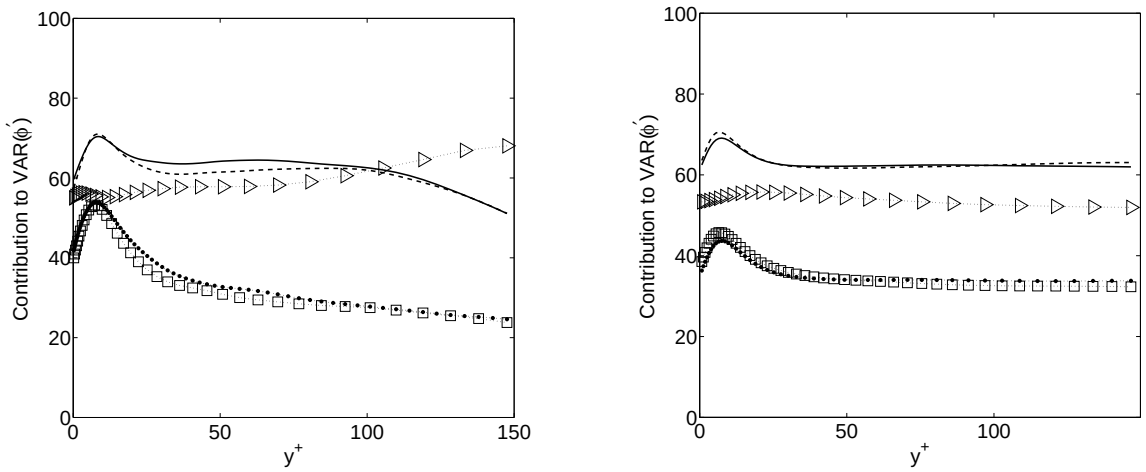

Figure 1: Percentage of $VAR(\phi')$ for events with different conditions. Solid line, $P(\widehat{\phi'^2} \geq k\phi^{+2}; \widehat{u'v'} < 0)$; $- - - - -$, $P(\widehat{\phi'^2} \geq k\phi^{+2}; \widehat{\theta'v'} < 0)$; $\bullet\!\!\cdot\!\!\bullet\!\!\cdot\!\!\bullet$, $P(\widehat{\phi'^2} \geq k\phi^{+2}; \widehat{u'v'} < 0; \widehat{v'} < 0)$; $\square.\square.\square.\square$, $P(\widehat{\phi'^2} \geq k\phi^{+2}; \widehat{\theta'v'} < 0; \widehat{v'} < 0)$; $\triangleright \cdot \triangleright \cdot \triangleright \cdot \triangleright$, $P(\widehat{\phi'^2} \geq k\phi^{+2}; \widehat{\partial p'/\partial x} > 0)$. (a) Channel flow; (b) Couette flow.

(III.b) Characterization of a wall-layer event associated with dissimilarity in non-perturbed turbulent flows

The relationship between $VAR(\phi')$ and those characteristic events in the wall layer responsible for the wall-normal turbulent transport was studied using conditional probability. The association of these events with the dissimilarity was evaluated by first detecting events that satisfy the condition $\widehat{\phi'^2} \geq k\phi^{+2}$, where ϕ^+ is a long-term statistic from a previous large sample, k is a parameter, and $\widehat{\phi'^2}$ is the variance of the dissimilarity during this event. Then, once an event with this condition was detected, which for simplicity was called an important dissimilarity event (IDE), a second (or even a third) condition (e.g., the sign of the wall-normal velocity $v' < 0$, etc.) was evaluated, and its dissimilarity $VAR(\phi')_{IDE}$ was evaluated. A detection algorithm, analogous to those used in the literature to detect burst or ejection events, was used (Blackwelder and Haritonidis, 1983; Johansson, Her and Haritonidis, 1987; Luchik and Tiederman, 1987). In this study, however, the goal was not to detect these kinds of events or evaluate the $VAR(\phi')$ associated with them. Rather, the goals were to detect a high amplitude in ϕ' greater than some value, or an IDE, checking whether it was, for example, an event in the second or fourth quadrant $(Q2 + Q4)$ according to the quadrant analysis technique, for Reynolds stress or wall-normal turbulent heat, etc., and to then evaluate its contribution to $VAR(\phi')_{IDE}$.

$$VAR = \widehat{\phi'^2} \; > \; k\phi^{+2} \tag{2}$$

where the mean, $\bar{\phi}$, and rms, ϕ^+, values used in previous condition (2) were long-term statistics, evaluated from a previous long sample, and the wide-hat symbol means a short term mean value in the T time filtering interval,

$$\widehat{\phi(t,T)^2} \; = \; \frac{1}{T}\int_{t-T/2}^{t+T/2} \phi(\tau)^2 d\tau \tag{3}$$

Then, once an event with condition (2) was detected, conditional probability with different conditions was applied to determine whether the IDE satisfied a second or a second and third condition. Some of the conditions included the following: $P(\widehat{\phi'^2} > k\phi^{+2}, \widehat{u'v'} < 0)$, to determine whether these events also belonged to events in the second or fourth quadrant $(Q2{+}Q4)$ for Reynolds stress; $P(\widehat{\phi'^2} > k\phi^{+2}, \widehat{u'v'} < 0, \widehat{v'} < 0)$, to determine whether these events also belonged to events in the fourth quadrant $(Q4)$ for Reynolds stress; or the condition $P(\widehat{\phi'^2} > k\phi^{+2}, \widehat{u'v'} < 0, \widehat{\theta'v'} < 0)$, to determine whether the dissimilarity associated with events in $(Q2 + Q4)$ for Reynolds stress was close to the dissimilarity associated with events in $(Q2 + Q4)$ for Reynolds stress and wall-normal turbulent heat at the same time. Figures 1(a) and 1(b) show some results from this algorithms.

(III.c) Natural dissimilarity in the frequency domain

Using the new variable the distribution of energy of the different spectra was evaluated. Fig. 2(a) and 2(b) show u', θ', p', and ϕ' spectra. These figures show that u' and θ' spectra present, for both flow configurations, a shift toward higher frequencies as the distance from the wall increase, being always more important for θ' than for u' (this behavior is clearer from the spectrum of their difference, ϕ').

(III.d) Velocity and temperature pressure-gradient interaction

There is a more significant correlation of θ' with $\partial p'/\partial x$ than u' with $\partial p'/\partial x$ (Figure 3). This correlation difference is the main cause of the dissimilarities in non-perturbed turbulent flows; or in the decorrelation of u' and θ' from the wall toward the central region.

IV. Dissimilarity in perturbed turbulent flows

(IV.a) Scheme of numerical simulations

To disrupt the mean-field analogy that exists in the developed conditions of the first DNS, different kinds of perturbations were used in a narrow region of the computational domain, or at the boundaries, of the

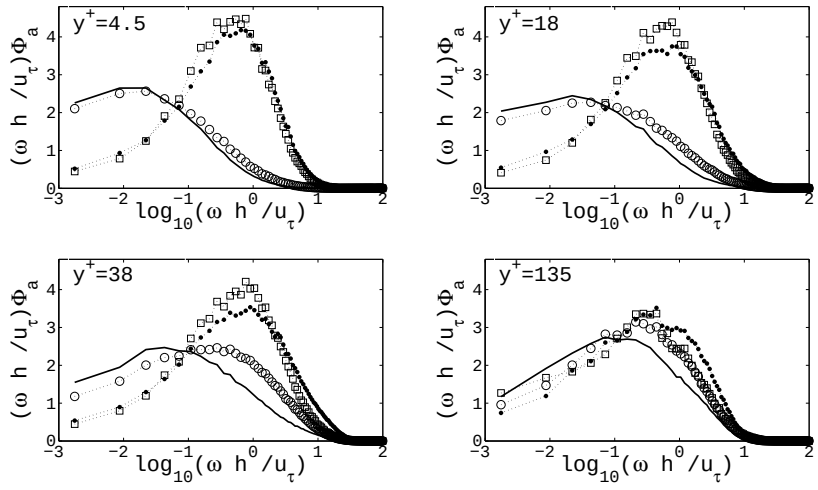

(a)

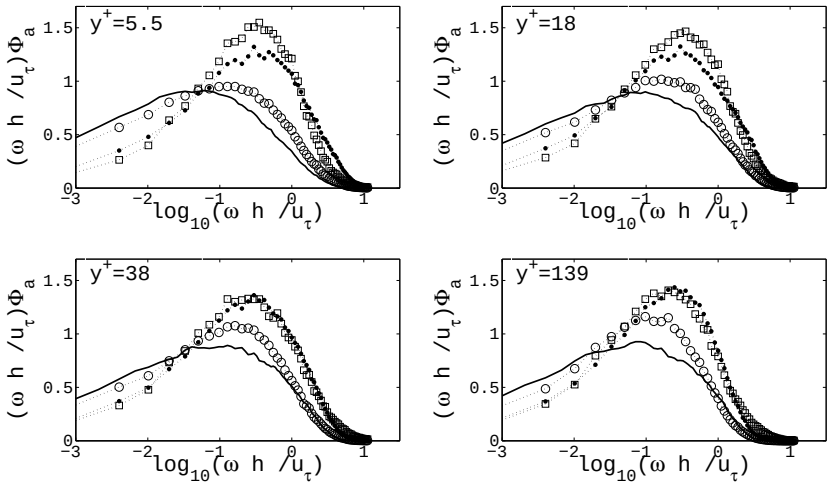

(b)

Figure 2: Spectral density functions of u', θ', ϕ', and p' at four positions from the wall for (a) channel and (b) Couette flow. Viscous region (top-left); buffer region (top-right); beginning of logarithmic region (bottom-left); center region (bottom-right). Solid line, $a = u'/u^+$; $\circ \cdot \circ \cdot \circ \cdot \circ$, $a = \theta'/\theta^+$; $\bullet .. \bullet .. \bullet$, $a = \phi'/\phi^+$; $\square.\square.\square.\square$, $a = p'/p^+$. Note the different scales.

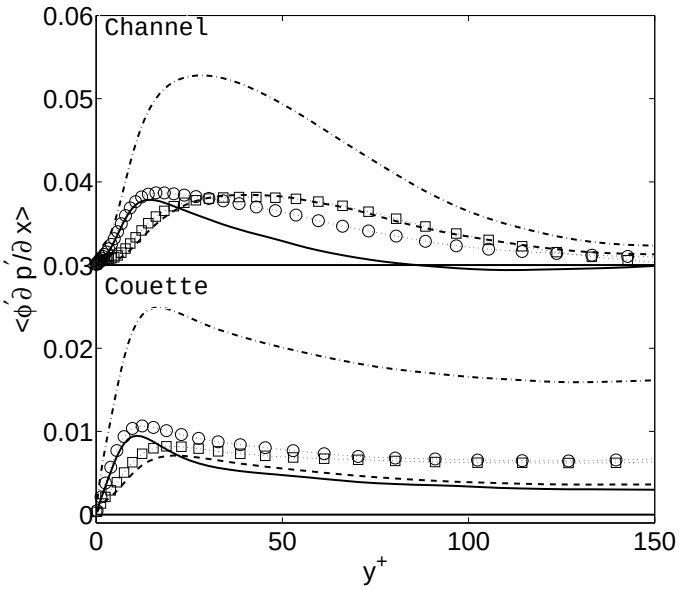

Figure 3: $-\langle\phi'\partial p'/\partial x\rangle$. $-.-.-.-.-$, total; solid line, at $Q4_{(u'v')}$; $-----$, at $Q2_{(u'v')}$; $\circ\cdot\circ\cdot\circ\cdot\circ$, $Q4_{(\theta'v')}$; $\square.\square.\square.\square$, $Q2_{(\theta'v')}$. Non-dimensionalized with u_τ^4/ν. Note the shift in the ordinate, 0.3, for the channel plot.

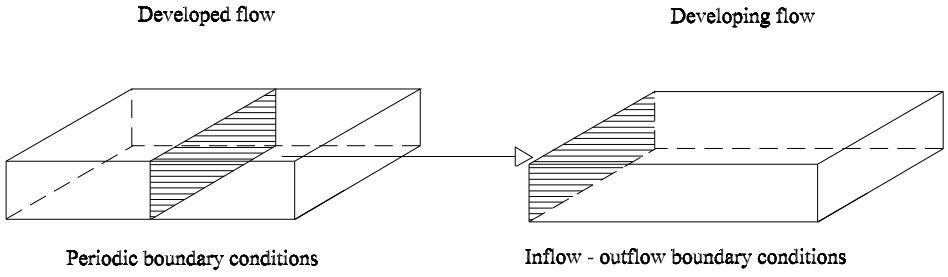

Figure 4: Scheme of parallel DNS for a numerical experiment of perturbed turbulent flow.

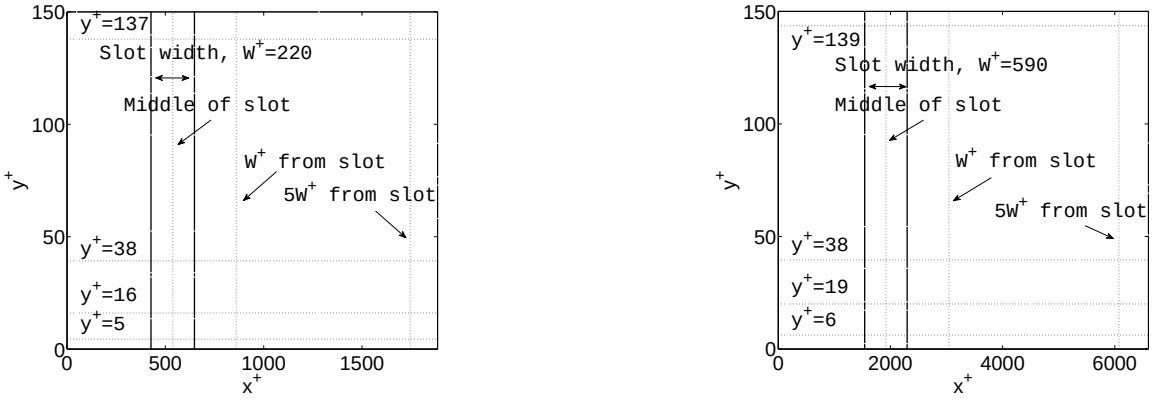

(a) (b)

Figure 5: Domain and location of spanwise slot used for perturbation. Solid vertical lines denote the slot location; vertical dotted lines denote sections where solution is presented, and horizontal dotted lines, positions from the wall where solution is presented. (a)Channel; (b)Couette flow.

second DNS. These perturbations were (a) local blowing and suction from a narrow span-wise slot at the wall, (b) local adverse and favorable streamwise pressure-gradient steps at a narrow span-wise volume of the buffer region, (c) local adverse and favorable wall-normal pressure-gradient steps at a narrow span-wise volume of the buffer region, and (d) local wall temperature steps.

The following is a list of the different numerical experiments reported in publications, which present the most important dissimilarity between turbulent fluxes.

1. CHB6220: Perturbed channel flow with blowing/suction from the lower wall, $W^+ = 220$, $v^+ = \pm 0.60$. Where W^+ is the width of the slot and v^+ the injected wall-normal velocity.

2. CFB6590: Perturbed plane Couette flow with blowing/suction from the lower wall, $W^+ = 590$, $v^+ = \pm 0.60$.

3. CHABR220: Perturbed channel flow with an adverse/favorable streamwise pressure-gradient step at the buffer region of the lower half, $W^+ = 220$, $(\partial P/\partial x)^+ = 0.30$ for adverse and -0.30 for favorable.

4. CFABR590: Perturbed plane Couette flow with an adverse pressure gradient step at the buffer region of the lower half, $W^+ = 590$, $(\partial P/\partial x)^+ = 0.18$ for adverse and -0.18 for favorable.

(IV.b) Leading contributor terms to turbulent fluxes dissimilarity

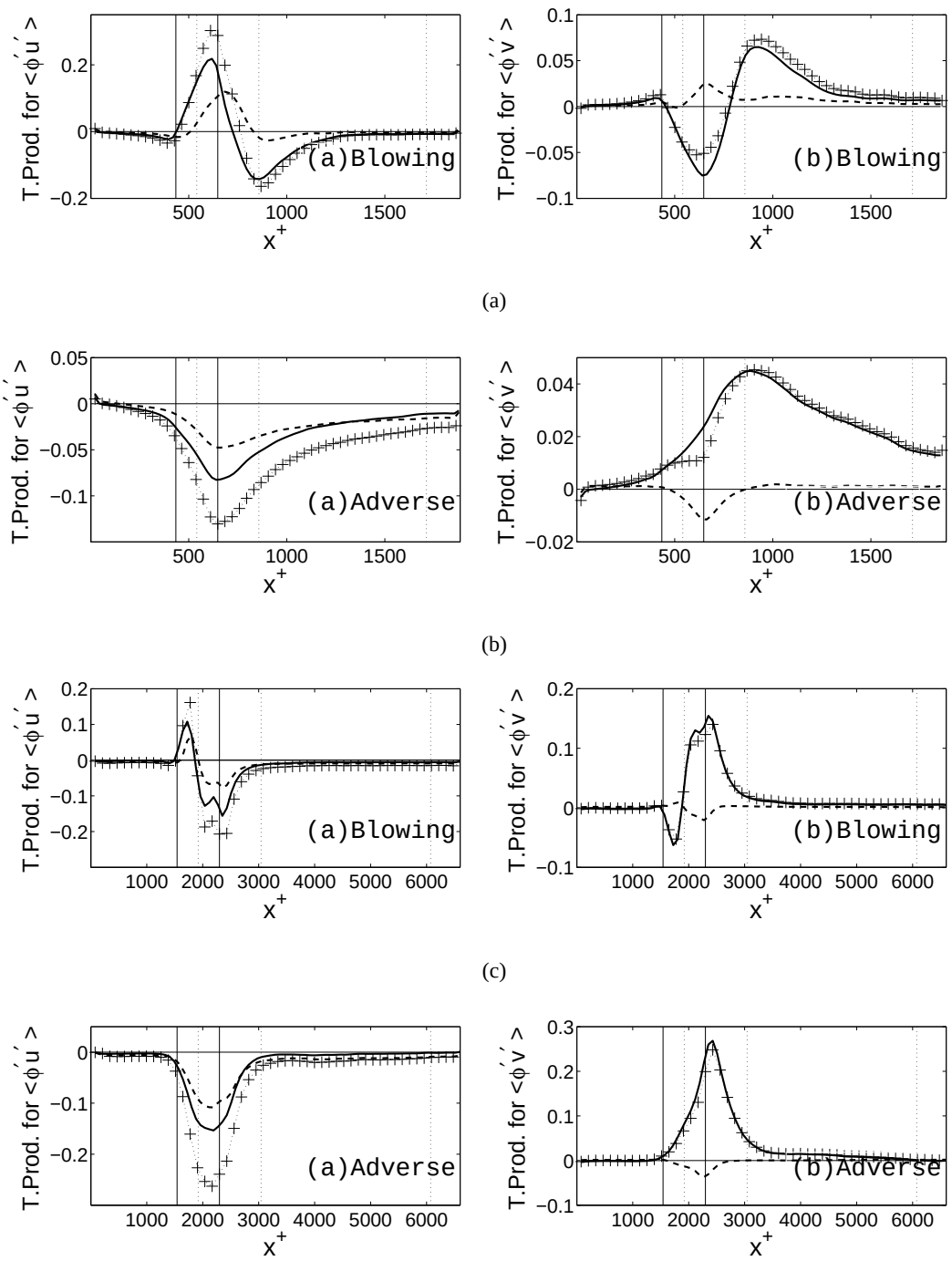

Figure 6: Contribution to differences $\langle \phi' u' \rangle$ (lhs) and $\langle \phi' v' \rangle$ (rhs) by turbulence production for cases (a) CHB6220, (b) CHABR220, (c) CFB6590, and (d) CFABR590 at $y^+ = 38$. $+ \cdot + \cdot + \cdot +$, total; solid line, function of mean-field dissimilarity; $- - - - -$, function of turbulence dissimilarity.

The differences between $(\langle u'u' \rangle - \langle \theta' u' \rangle)$ depend primarily on mean flow, and secondarily on turbulence, with $\langle u'v' \rangle \partial\Phi/\partial y$ as the leading term. Conversely, the differences between $(\langle u'v' \rangle - \langle \theta' v' \rangle)$ depend mostly on mean flow dissimilarity, with $\langle v'v' \rangle \partial\Phi/\partial y$ as the leading term. In other words mean fields wall-normal gradients play the most important rule in the dissimilarity between streamwise velocity and temperature mean turbulent fluxes. Figures 6(a), 6(b), 6(c), 6(d) show these results for blowing and adverse pressure gradient step for both flow configurations. In those regions of the flow where $\partial\Phi/\partial y = \partial U/\partial y - \partial\Theta/\partial y = 0$ dissimilarity is minimal. Both flow configurations, channel and Couette flow, present similar results.

(IV.c) A relation that holds for non-perturbed and perturbed turbulent flow

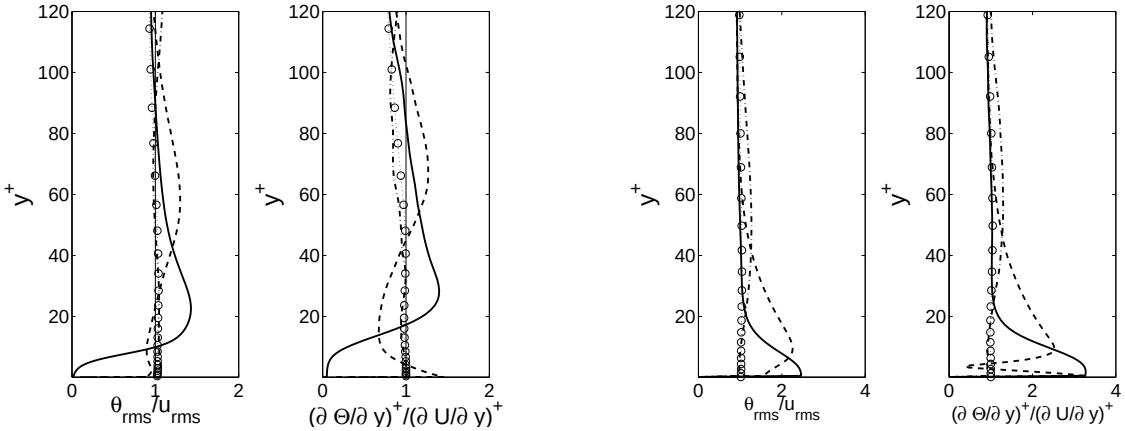

(a) (b)

Figure 7: θ_{rms}/u_{rms} and $(\partial\Theta/\partial y)/(\partial U/\partial y)$ for channel flow perturbed with (a) blowing and (b) temperature step at the wall. $\circ \cdot \circ \cdot \circ \cdot \circ$, non-perturbed values. Solid line, on the slot; $- - - - -$, W^+; $-.-.-.-.-$, $5W^+$ downstream.

For $Pr = 1$ the following relation holds for the wall-layer for the simple non-perturbed and perturbed turbulent flows used in this study (Figures 7(a) and 7(b)):

$$\frac{u_{rms}}{\partial U/\partial y} \simeq \frac{\theta_{rms}}{\partial\Theta/\partial y} \tag{4}$$

(IV.d) Turbulent heat transfer modeling

The following transformations of the Reynolds stresses using the wall-normal gradients of streamwise velocity and temperature show a reasonable *a priori* predictions of the turbulent heat fluxes, as it is shown in Figures 8(a) and 8(b), for both flow configurations.

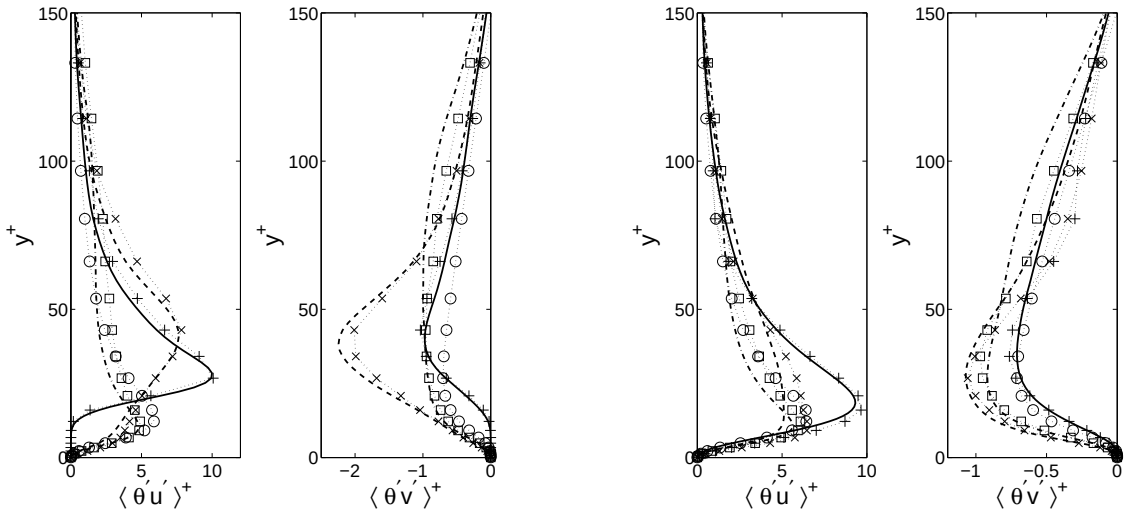

(a) (b)

Figure 8: *A prior* comparison of modeled turbulent heat flux $\langle\theta' u'\rangle^+$ and $\langle\theta' v'\rangle^+$, for channel flow perturbed with (a) blowing and (b) an adverse axial pressure gradient step. Solid line, and $+\cdot+\cdot+\cdot+$(second symbol modeled), on the slot; $---$, and $\times\cdot\times\cdot\times\cdot\times$, W^+; $-.-.-.-.-$, and $\square.\square.\square.\square$, $5W^+$ downstream; $\circ\cdot\circ\cdot\circ\cdot\circ$, non-perturbed values.

$$\langle\theta' u'\rangle \;\simeq\; \langle u' u'\rangle \,\frac{\theta_{rms}}{u_{rms}} \;\simeq\; \langle u' u'\rangle \frac{\partial\Theta/\partial y}{\partial U/\partial y} \tag{5}$$

and,

$$\langle\theta' v'\rangle \;\simeq\; \langle u' v'\rangle \,\frac{\theta_{rms}}{u_{rms}} \simeq\; \langle u' v'\rangle \frac{\partial\Theta/\partial y}{\partial U/\partial y} \tag{6}$$

where all variables are in dimensionless form.

References

1. R.A. Antonia, L.V. Krishnamoorthy, and L. Fulachier. Correlation between the longitudinal velocity fluctuation and temperature fluctuation in the near-wall region of a turbulent boundary layer. *Int. J. Heat Mass Transfer*, **31**(4), 723-730, 1987.

2. R.F. Blackwelder and J.H. Haritonidis. Scaling of the bursting frequency in turbulent boundary layers. *J. Fluid Mech.*. **132**, pp. 87, 1983.

3. L. Fulachier and R. Dumas. Spectral analogy between temperature and velocity fluctuations in a turbulent boundary layer. *J. Fluid Mechanics*, **77**, 257-277, 1976.

4. A.V. Johansson, J.Y. Her, and J.H. Haritonidis. On the generation of high-amplitude wall-pressure peaks in turbulent boundary layer and spots. *J. Fluid Mech*, **176**, pp. 119-142, 1987.

5. J. Kestin, and P.D. Richardson. Heat transfer across turbulent incompressible boundary layers. *Int. J. Heat Mass Transfer*, **6**, 147-189, 1963.

6. H. Kong, H. Choi, and J.S. Lee.Dissimilarity between the velocity and temperature fields in a perturbed turbulent thermal boundary layer. *Physics of Fluids*, **13**(5), 1466-1479, 2001.

7. T.S. Luchik and W.G. Tiederman. Timescale and structure of ejections and bursts in turbulent channel flows *Journal of Fluid Mechanics*. **174**, 529-552, 1987.

Publications acknowledging AFOSR support resulting from this grant (published and submitted)

1. H.D. Pasinato. Velocity and Temperature Dissimilarity in Fully Developed Turbulent Channel and Plane Couette Flows, *Int. J. Heat and Fluid Flow*, **32**, pp. 11-25, 2011.

2. H.D. Pasinato. Streamwise Velocity and Temperature Dissimilarity in Perturbed Turbulent Flows, to be submitted.

3. Pasinato, H.D., 2007, *Velocity and Temperature Natural Dissimilarity in a Turbulent Channel Flow*, *Mecánica Computacional*, Vol. **XXVI**, pp. 3644-3663, Ed. by Elaskar, S.A., E.A. Pilotta, and G.A. Torres.

   (http://venus.ceride.gov.ar/twiki/bin/view/AMCA/ListadoDePublicaciones).

4. Pasinato, H.D. 2008, Turbulent Scalar Transport Mechanism and Velocity-Temperature Natural Dissimilarity in a Turbulent Plane Couette Flow, In *Mecánica Computacional* Vol. XXVII, Ed. by A. Cardona, M. Storti, and C. Zuppa, pp.1619-1636, 2008,

   http://venus.ceride.gov.ar/twiki/bin/view/AMCA/ListadoDePublicaciones).

5. H.D. Pasinato. Large-Eddy Simulation of the Flow and Thermal Fields Past a Circular Cylinder , In *Mecánica Computacional* Vol. XXVII, Ed. by A. Cardona, M. Storti, and C. Zuppa, pp.249-264, 2008.

   http://venus.ceride.gov.ar/twiki/bin/view/AMCA/ListadoDePublicaciones).